Current Eye Research

ISSN: 0271-3683 (Print) 1460-2202 (Online) Journal homepage: http://www.tandfonline.com/loi/icey20

Relative Peripheral Myopia Induced by Fractal Contact Lenses

Manuel Rodriguez-Vallejo, Diego Montagud, Juan A. Monsoriu, Vicente Ferrando & Walter D. Furlan

To cite this article: Manuel Rodriguez-Vallejo, Diego Montagud, Juan A. Monsoriu, Vicente Ferrando & Walter D. Furlan (2018): Relative Peripheral Myopia Induced by Fractal Contact Lenses, Current Eye Research, DOI: 10.1080/02713683.2018.1507043

To link to this article: https://doi.org/10.1080/02713683.2018.1507043

Published online: 08 Aug 2018.

CURRENT EYE RESEARCH
https://doi.org/10.1080/02713683.2018.1507043

Taylor & Francis
Taylor & Francis Group

Relative Peripheral Myopia Induced by Fractal Contact Lenses

Manuel Rodriguez-Vallejo [a], Diego Montagud[b], Juan A. Monsoriu[b], Vicente Ferrando[c], and Walter D. Furlan[c]

[a]Department of Ophthalmology (Qvision), Vithas Virgen del Mar Hospital, Almería, Spain; [b]Centro de Tecnologías Físicas, Universitat Politècnica de València, Valencia, Spain; [c]Departamento de Óptica, Universitat de València, Burjassot, Spain

ABSTRACT

Purpose: To assess the peripheral refraction induced by Fractal Contact Lenses (FCLs) in myopic eyes by means of a two-dimensional Relative Peripheral Refractive Error (RPRE) map.

Materials and Methods: This study involved 26 myopic subjects ranging from −0.50 D to −7.00 D. FCLs prototypes were custom-manufactured and characterized. Corneal topographies were taken in order to assess correlations between corneal asphericity and lens decentration. Two-dimensional RPREs were measured with an open-field autorefractor at 67 points, covering the central 60 × 30 degrees of the visual field. The bidimensional RPRE vector components: M, J_0 and J_{45} of the difference between the values obtained with and without the FCLs in the eye were obtained. Additionally, the FCL-induced peripheral refraction in tangential and sagittal planes was computed along the horizontal meridian.

Results: Induced by the FCLs, significant differences for all vector components were found in the peripheral retina. FCLs were decentered a mean of 0.7 ± 0.19 mm to the temporal cornea. The two-dimensional RPRE maps manifested the FCLs decentration. In particular, M varied asymmetrically between nasal and temporal retina after fitting the FCLs with a significant increment of the myopic shift beyond 10º ($p < 0.05$). No correlations were found between the amount of lens decentration and the asphericity of the cornea along temporal and nasal sides. However, significant correlations were found between the corneal asphericity and vector components of the RPRE in naked eyes. FCLs produced an increasing myopic shift in tangential and sagittal power errors along the horizontal meridian.

Conclusions: As predicted by ray-tracing simulations, FCLs fitted in myopic eyes produce a myopic shift of the RPRE. The two-dimensional RPRE maps show information about the lens performance that is hidden in the conventional one-dimensional meridional representations.

ARTICLE HISTORY
Received 3 February 2018
Revised 17 July 2018
Accepted 28 July 2018

KEYWORDS
Myopia progression; contact lenses; fractal; peripheral refractive error; two-dimensional maps

Introduction

During the last few years myopia control therapies have deserved a large interest among researchers and vision care professionals.[1–3] Several methods have been proposed to slow myopia progression. Among them, non-pharmacological treatments, like orthokeratology[4] and peripheral defocus modifying contact lenses (CLs)[5] achieved very good outcomes. Although the optical mechanisms for myopia development still remain controversial,[6,7] these results have been mainly attributed to a myopic Relative Peripheral Refractive Error (RPRE) induced by the lenses. Consequently, different designs of multifocal CLs with different amount and extension of the induced RPRE were proposed to this aim.[8–10] Since the ocular growth during the emmetropization process might depend on the stimulated retinal areas,[11] it is expected that different designs will provide disparate results. Therefore, to obtain information about RPRE induced by different lenses in the spherical, but also in the astigmatic component of the refraction, across the whole paracentral retina seems to be of great importance to understand the lens success in myopia progression. In particular, it is likely that the astigmatic component of the RPRE plays a role in the myopia development in humans, as it has been demonstrated it plays in the emmetropization in monkeys[12] and chicks.[13]

In a previous paper,[10] we have proposed a new design of CLs for myopia control, named Fractal Contact Lenses (FCLs). The potentiality of FCLs to produce a myopic RPRE was demonstrated by ray tracing methods in model eyes. However, the good theoretical performance obtained with FCLs has not been still validated in real eyes. Therefore, the main aim of this study is to assess the peripheral refraction induced by FCLs. To do that, FCLs prototypes were specially manufactured and characterized. In order to obtain a complete assessment of the lens performance in real myopic eyes, we measured the RPRE induced by the lenses at 67 locations across the 60º x 30º of right eye visual field with an open field autorefractometer. The mean values of the measured dioptric power vectors (M, J_0, and J_{45}), were represented as contour plots in 2D power maps. In this sense, our approach improves the assessment methods employed in previous works evaluating contact lenses,[3,4] because we are able to obtain complete 2D information about the induced RPRE at different positions of the visual field.

CONTACT Manuel Rodriguez-Vallejo manuelrodriguezid@qvision.es Department of Ophthalmology (Qvision), Vithas Virgen del Mar Hospital, Almería, Spain
Color versions of one or more of the figures in the article can be found online at www.tandfonline.com/icey.

Materials and methods

Contact lenses construction and characterization

FCLs are multizone bifocals in which the zones are radially distributed following a fractal sequence.[10] Specifically, we employed the fractal triadic Cantor set, which has also been applied to define diffractive lenses known as Fractal zone plates.-[14] The FCL design is summarized in Figure 1. The fractal triadic Cantor set is constructed sequentially from a straight-line segment of unit length (see Figure 1A), called *initiator* (stage $S = 0$). Next, at stage $S = 1$, the *generator* of the set is created by dividing the segment into 3 equal sub segments of length $x = 1/3$ and removing the central one. Then, this procedure is continued at the subsequent stages, $S = 2, 3\ldots$, on each sub segment. At this point, a change of variables $r = b\sqrt{(x)}$ is performed to define the extension of the concentric zones in the FCL, up to a given lens radius b (see Figure 1B). As FCLs are designed with S = 2; seven fractal zones, distributed along the square of the radial coordinate, are defined in its surface.[10] The theoretical profile of a FCL is shown in Figure 1C. As can be seen, the lens alternates two different radii of curvature corresponding to far (center) and near (therapeutic) powers.

Following the design shown in Figure1C, a set of FCLs prototypes were manufactured by Lenticon SA (Tres Cantos, Spain) using a precision lathe (Optoform 40, Sterling Ultra Precision, Largo, USA). The lenses had a labeled treatment power of + 2.00 D and correction powers ranging from −0.50 D to −7.00 D in −0.50 D steps, The lens material was Hioxifilcon A (Benz G5X p-GMA/HEMA), whose refractive index, hydrated and at 35º, is 1.401. Each FCLs model was manufactured with a diameter of 14.50 mm and two different base curves: 8.4 mm and 8.6 mm. The constructed lenses (28 FCLs in total) were assessed with the Nimo TR1504 (LAMBDA-X, Nivelles, Belgium) contact lens power mapper (version 4.2.6.0 r477). The instrument software allows to obtain the dioptric power profiles of multifocal CLs, however it is not able to locate the zones in a multizone CLs and it is the operator who must enter the radii of the zones (with a maximum of five zones). For this reason, we developed a custom software using MATLAB (Mathworks, Inc., Natwick, MA) to precisely detect the power transition between therapeutic and compensation zones.[15] The algorithm computes the second derivative of the dioptric power profile exported from the NIMO, and shows the transition between two zones of different power (see Figure 2A). The program also obtains the parabolic profiles of both the base (far distance) power of the lens and its therapeutic power (see Figure 2B). For a given radius ρ of the pupil, the fourth-order Zernike spherical aberration of the lens: $C_{4,0}$ is obtained by fitting the profile to a parabolic curve $P(r) = P_0 + br^2$ as: $C_{4,0} = b\,\rho^4/24\sqrt{5}$ where P_0 is the paraxial power (at r = 0). [16] By using this method, each lens was relabelled with its true (experimental) therapeutic and correction power.

Subjects and procedures

The research adhered to the tenets of the Declaration of Helsinki. All participants gave written consent after explanation of the nature of the study, which was approved by the Institutional Review Board of the University of Valencia. Twenty-six myopic subjects (mean age 23.77 ± 3.62 years) participated in this study (18 females and 8 males). All participants underwent a complete eye exam including objective and subjective refraction and slit-lamp exploration. Only right eyes were considered. Inclusion criteria were: myopic eyes ranging from −0.50 D to −7.00 D (mean −2.62 ± 1.59 D) and astigmatism ≤ 0.75 D, with no ocular diseases, strabismus or amblyopia, and with corrected distance visual acuity better than 0.2 log MAR.

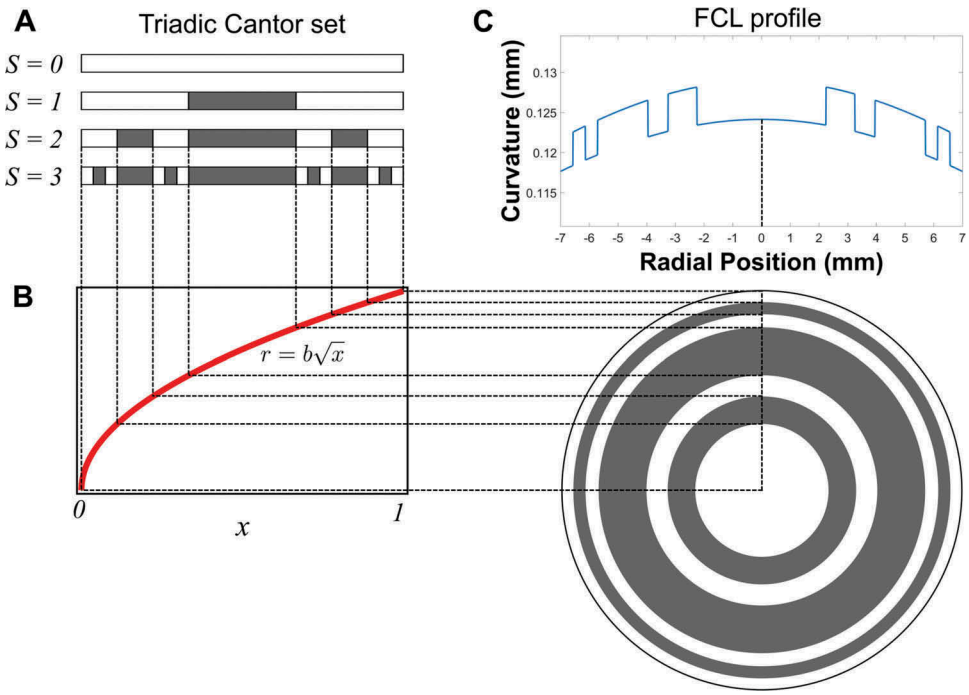

Figure 1. FCL design. A, Triadic Cantor set developed up to three steps, $S = 3$. B, FCL fractal zones distribution for $S = 2$, obtained through the coordinate transformation $r = b\sqrt{(x)}$. C, FCL surface profile.

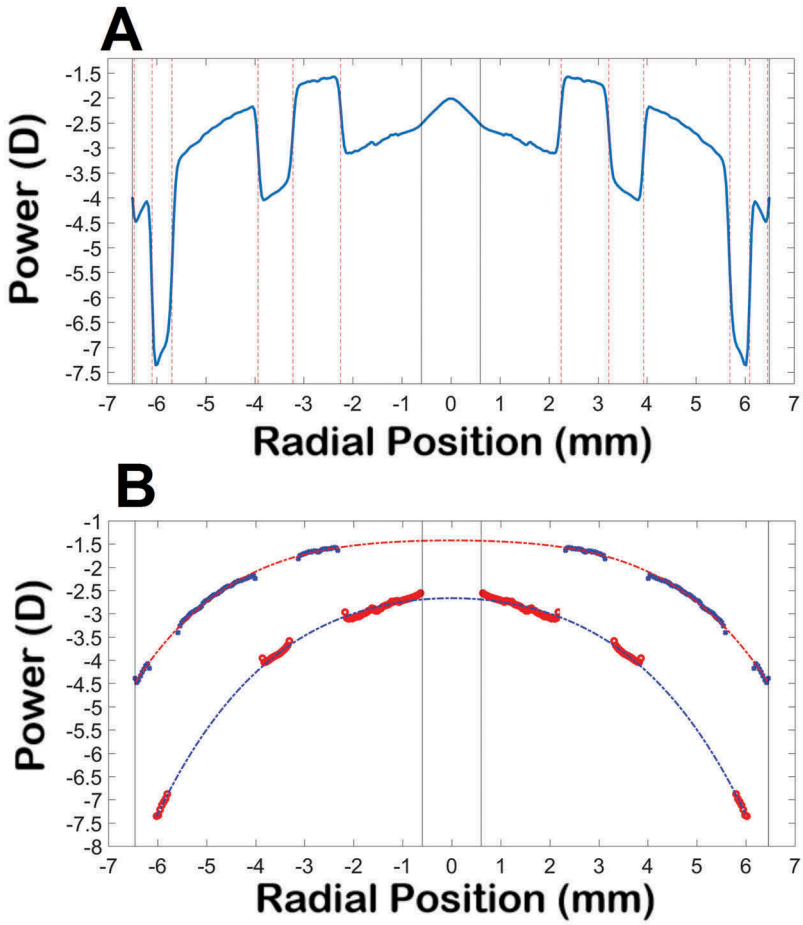

Figure 2. A, Measured zones in a constructed FCL with mean far power −3.5 D. Vertical lines are the limits of the zones detected by the custom software (see Ref. [15]). B, Radial variation of the base and treatment powers fitted to a parabolic radial profile reflecting the spherical aberration of the lens. In this case, for a 6 mm lens diameter, the values of spherical aberration Zernike coefficient was $C_{4,0}$ = −0.012 µm for the base profile.

Before fitting the FCLs, corneal topographies were taken on the naked eye with the Keratron Scout topographer (Optikon 2000 SpA, Rome, Italy). Elevation data were exported in binary format, and a custom software was programmed in MATLAB in order to compute corneal asphericities at the nasal and temporal sides, along the horizontal (0º–180º) meridian, fitting elevation data to a conic function.[17]

Each subject was fitted with the FCL of the constructed set having the compensation power closer to the spectacle refraction after correction of vertex distance power, and with the base curve that best matched the corneal radius. The behavior of the lenses, movement, and centration were evaluated by the examiner 20 minutes after fitting. Then corneal topographies were taken again but with the patient wearing the best fitted FCL. The distance from the center of the first therapeutic zone and the center of the pupil diameter was measured with the caliper tool of the Keratron Scout software to obtain the FCL decentration in each case.

Peripheral refractive error

Objective central and peripheral refractions were measured with an open-field autorefractor (Grand-Seiko WAM-5500, Grand-Seiko Co., Ltd., Hiroshima, Japan). All measurements were made in non-cyclopegic conditions at environmental mesopic light conditions to ensure minimum pupil diameters of 4 mm in all participants.

Participants looked at 67 fixation targets (high contrast circles of 25.4 mm diameter located on a 2 m distant wall) covering 60º x 30º of the central visual field, see Figure 3. Measurements were taken with the eye rotation technique,[18] and the alignment was achieved with the instrument alignment camera, so that the pupil of the tested eye was centered with respect of the measuring axis. Participants fixated the targets sequentially from left to right, line by line from the top. Refractions in clinical notation (sphere, cylinder and axis) were exported for analysis in MATLAB code. Each measure was converted to vector components: spherical equivalent M, with/against the rule astigmatism: J_0, and oblique astigmatism: J_{45}.[19] The program requests the examiner to obtain a minimum of three averaged measures per fixation point up to having standard deviations lower than 0.3 D, and automatically calculates the mean values of M, J_0, and J_{45}. The data collection process to obtain a full 2D peripheral refractive map of an eye took around 10–12 minutes. The RPRE was measured in each subject first with the naked eye (baseline state) and then in the same eye fitted with the FCL. The RPREs were calculated by subtracting the central values of each vector component from the corresponding peripheral one. Contour maps representing the mean values of M, J_0

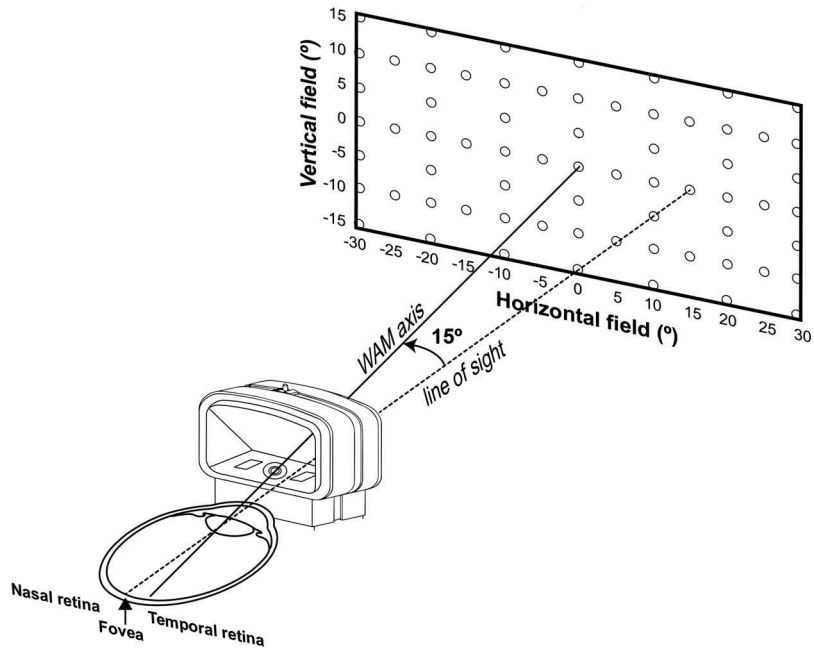

Figure 3. Schematic representation of the right eye RPRE measurement with WAM-5500 . The circles represent the discrete points measured with the eye rotation method.

and J_{45} at each visual field location were generated using cubic interpolation in steps of 0.5 degrees. Recorded data was used to compute also the tangential ($F_T = M + J_0$) and sagittal ($F_S = M - J_0$) power errors along the horizontal meridian.

Statistical analysis

Statistical analysis was done using SPSS software version 20 (SPSS Inc., Chicago, IL, USA), $p < 0.05$ was considered to indicate significance. Normal distributions were tested with the Shapiro-Wilk test. Paired t-tests were used to analyze the differences between the RPRE vector components obtained with the FCLs and with the naked eye. To investigate the potential role that the corneal asphericity plays in the RPRE, Pearson correlation analyses were performed to determine the relationship between these two parameters. Power analysis was performed using G Power version 3.1.9.2 (available at http://www.gpower.hhu.de/). The sample size in this study offered 88% statistical power at a 5% level to detect a difference in RPRE of 0.25 D with and without FCLs when the expected standard deviation (SD) of the mean difference was 0.44 D.

Results

Contact lenses: power profiles and fitting

The power profiles of the therapeutic zones of the constructed lenses had a mean value of 1.32 ± 0.28 D, which resulted 0.68 D lower than the theoretical labeled + 2.00 D power. The compensation power of the FCL prototypes was negatively correlated with the experimental therapeutic power ($r = -0.786$, $p = 0.007$); that is; in the prototypes, we found that the higher the absolute value of the compensation power, the lower the therapeutic power of the lens.

When fitted in patients, topological data revealed that CLs were decentered (related to the pupil center) toward temporal cornea, ranging from 0.39 mm to 1.05 mm (mean 0.7 ± 0.19 mm) whereas mean vertical displacement was 0.00 ± 0.49 mm (ranging from 0.64 mm down to 1.38 mm up). The mean value of the pupil entrance diameter was 3.67 ± 0.53 mm measured with the Keratron in the naked eye. See Figure 4.

The mean values of the corneal asphericities along a 4 mm semi-chord in the horizontal meridian were −0.07 ± 0.09 and −0.24 ± 0.18 for the temporal and nasal cornea respectively.

No correlations were found between the amount of lens decentration and the asphericity of the cornea along temporal and nasal sides.

Relative peripheral refractive error

Significant correlations were found between the corneal asphericity and vector components of the RPRE at several points along the horizontal meridian in the naked eye. These values are reported in Table 1.

Baseline mean values of the RPRE for M, J_0 and J_{45} are represented in Figure 5A, 5D and 5G, respectively. Figure 5B, 5E, and 5H show the mean values for the same eyes wearing FCLs. The net effect of the lens is shown in Figure 5C, 5F, and 5I. In these plots, crosses were drawn at those positions where the myopic RPRE induced by the FCL was statistically significant. It can be seen that the mean myopic shift induced by FCLs increases with the eccentricity and becomes significant ($p < 0.05$) at 10° in the temporal retina (nasal visual field). Note that refractive components obtained with the lens fitted to the eyes reflect the lens decentration to the temporal cornea. In fact, the effect of the FCL on the spherical equivalent M was almost uniform around the center of the lens (see Figure 5B),

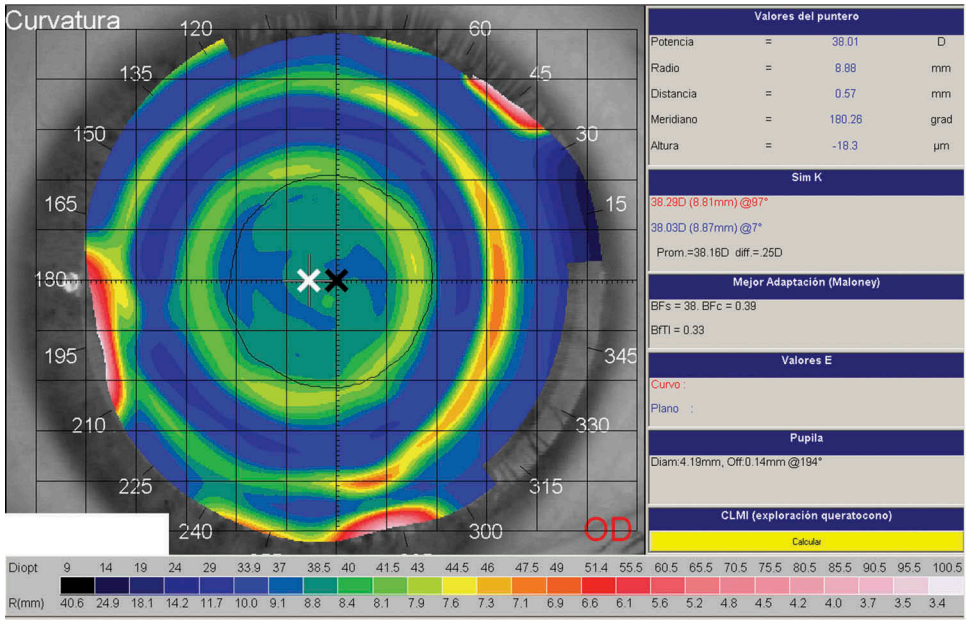

Figure 4. Topographic image of the FCL fitted in a patient's eye. Black and white crosses indicate the centers of the pupil and the lens respectively. In this case a decentration of 0.57 mm was measured.

Table 1. Correlations between Relative Peripheral Refractive Error (RPRE) vector components and corneal asphericity at the Temporal or Nasal semi-chord of the cornea from the normal vertex to 4 mm of radial position in the naked eye. Only significant values are included.

Retinal Area (°)	RPRE (D) Mean ± SD	Corneal side	Pearson r
M			
−25 (NR)	−0.22 ± 0.47	Temporal	−0.452, p = 0.040
−15 (NR)	−0.21 ± 0.40	Temporal	−0.526, p = 0.014
−10 (NR)	−0.27 ± 0.29	Temporal	−0.436, p = 0.048
J0			
+ 25 (TR)	−0.82 ± 0.29	Nasal	−0.572, p = 0.007
+ 20 (TR)	−0.56 ± 0.22	Nasal	−0.562, p = 0.008
+ 10 (TR)	−0.1 ± 0.2	Nasal	−0.505, p = 0.019
J45			
+ 30 (TR)	0.11 ± 0.25	Nasal	−0.581, p = 0.006
+ 20 (TR)	0.05 ± 0.15	Nasal	−0.465, p = 0.033
+ 10 (TR)	−0.01 ± 0.09	Nasal	−0.478, p = 0.028
+ 5 (TR)	0.01 ± 0.09	Nasal	−0.467, p = 0.033

NR = Nasal retina; TR = Temporal retina.

while, as expected, affects mainly the horizontal and vertical meridians for the J_0 component and the same for the J_{45} component in oblique meridians for (see Figure 5E and 5H).

Figure 6A shows the spherical equivalent (M) measured along the horizontal meridian, both, at the baseline state and with the FCLs. An increase of the myopic shift was found with the FCLs at the temporal retina from 10° to 30° ($p < 0.05$). We found that the myopic shift (M) induced by the FCLs at 25° and 30° in the temporal field decreased with the lens decentration through the temporal side of the cornea r = 0.50 (p = 0.013) at 25° and r = 0.54 (p = 0.006) at 30°. In the same figure we have plotted the numerical result obtained on the Atchison Model Eye 1 (with −2.00 D refractive error) using a ray tracing software.[10] The model eye was fitted with a FCL of −2.00D, having therapeutic zones of 1.32 D (the mean value obtained for the constructed lenses), and decentered 0.7 mm, which was the mean value of lens decentration on the eyes. As the model eye is axially symmetric, it cannot reflect the asymmetry of RPRE on the temporal and nasal field observed in the experiment, therefore, only the temporal data of the numerical simulations was represented in this figure. An excellent agreement can be observed between numerical[10] and experimental results.

Tangential and sagittal power errors along the horizontal meridian are shown in Figure 6B and 6C. As can be seen the FCLs produce an increasing myopic shift in the F_T curve, with a maximum value at 20° of the temporal retina. F_S also reveals a myopic shift with the FCL, even though less markedly than F_T, but highly enough to move the sagittal foci to the front of the retina.

Discussion

Derived from experimental studies in animals, that found that the refractive error in the peripheral retina can regulate the eye growth, current successful treatments aimed to slow myopia progression, such as ortokeratology or multifocal contact lenses are intended to create a relative peripheral myopia. In most of the clinical studies, the study of the effect of the proposed solutions was restricted to the analysis of the RPRE, measured in terms of vector components M, J_0 and J_{45} along the horizontal meridian,[3] and only few include the vertical and oblique meridians.[20,21]

In this work we have presented the first clinical study in which the ability of a new design of contact lenses[10] to create a RPRE in the whole 2D visual field has been demonstrated. Taking into account that, on the one hand, the mean power at the treatment zones (+ 1.32 D) of the manufactured lenses was lower than the theoretical labeled power (+ 2.00 D); and, on the other hand, that lens prototypes were decentered during the RPRE measurements, an excellent agreement between the theoretical and experimental results has been obtained (see Figure 6A).

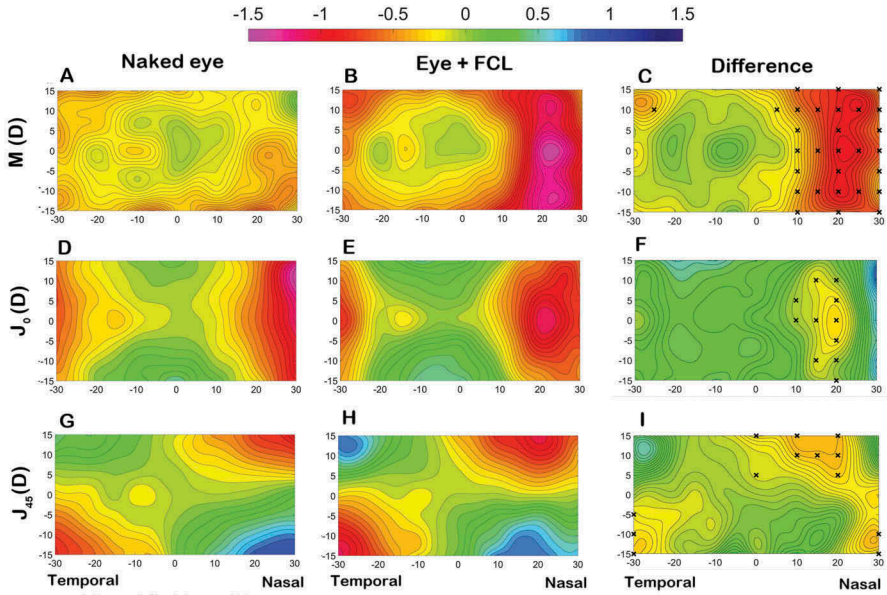

Figure 5. Mean values of the relative peripheral refractive error (RPRE) across the visual field for the vector components M, J_0 and J_{45}, at the baseline state (left); with FCLs fitted in the eye (center) and the difference (right). Temporal and Nasal refer to the right eye's field of view that has correspondence to the Nasal and Temporal retinal locations respectively. Crosses in the right column indicate field positions (see Figure 3) where the myopic RPRE induced by the FCL is statistically significant ($p < 0.05$).

In the assessment of the prototypes, we found a negative correlation between the compensation power and the power at the therapeutic zones, which means that high power minus lenses had less power in the therapeutic zones, than low power FCLs. This effect, that can be attributed to the spherical aberration, should be taken into account in future studies, since as we have shown in our theoretical model, higher degrees of myopia should need higher treatment powers. In FCLs, this limitation could be easily solved since the treatment power this is a free design parameter.[10]

For the naked eye, we found that corneal asphericity along temporal and nasal semichords in the horizontal meridian was negatively correlated with the M component; but only for temporal cornea and nasal retina whereas for J_{45} and J_0 the negative correlations where found between nasal cornea and temporal retina (Table 1). This is also in agreement with theoretical models, which assert that, the more positive the asphericity Q value, the more myopic the peripheral refraction induced for M and J_0.[22–24] For the naked eye, the sample showed a relative peripheral myopia lower than −0.50 D for M. We also found a trend for J_0 to become more negative in both sides of the retina, whereas J_{45} becomes more negative with increasing eccentricity in the superior-nasal to inferior-temporal visual field. These results agree with those reported in previous studies that measured peripheral M and oblique astigmatism in myopes with a Hartmann-Shack aberrometer. [6,25]Moreover, we found that the typical asymmetry in the astigmatic components of RPRE measured in naked eyes, which can be explained by angle lambda (see for instance Ref.[26] and references therein), was enhanced by the FCLs power, as can be seen in Figure. 5B, 5E, and 5H. Additionally, note in these plots that the lens decentration induced a shift of the maps to the temporal side of the visual field. On the other hand, in our sample the sagittal focus was hyperopic in the naked eye along the nasal visual field (Figure 6C), but became myopic with the FCLs. This effect has not been observed in the relative RPRE induced by ortokeratology.[4]

The limitations of this work mainly rely in the FCL fitting during the experiment. First, we cannot predict precisely how the lens moves and fits on the eye during eye rotations. However, we decided to adopt the eye rotation technique because, being less time consuming, and also closer to everyday life viewing situations, it provided no significant differences with the head rotation technique. [18] Second, the lens centration affected the results of the RPRE. However, we have shown that this effect is highly predictable with our model, and therefore, taking into account that lens centration can be corrected by modifying the design of the lens base curve, thickness, and/or increasing the total diameter, an optimization of these parameters should be considered in future designs.

In conclusion, in this work we have experimentally validated ability of the FCLs to create a myopic RPRE in myopic eyes. We also have confirmed that, considering both, the imperfections in the manufacturing process of the prototypes, and the lens decentration, the theoretical model used in Ref. [10] can accurately be used to predict the lens effect in real eyes.

On the other hand, the new two-dimensional representation of the RPRE employed here to study the effect of the lens in different areas of the visual field, offered us further information about what happens in a wide area of the retina, especially considering the lens decentration. This means that this representation is convenient for increasing the knowledge about the changes in the astigmatism components induced by the lenses. For instance, we found that for the J_{45} component

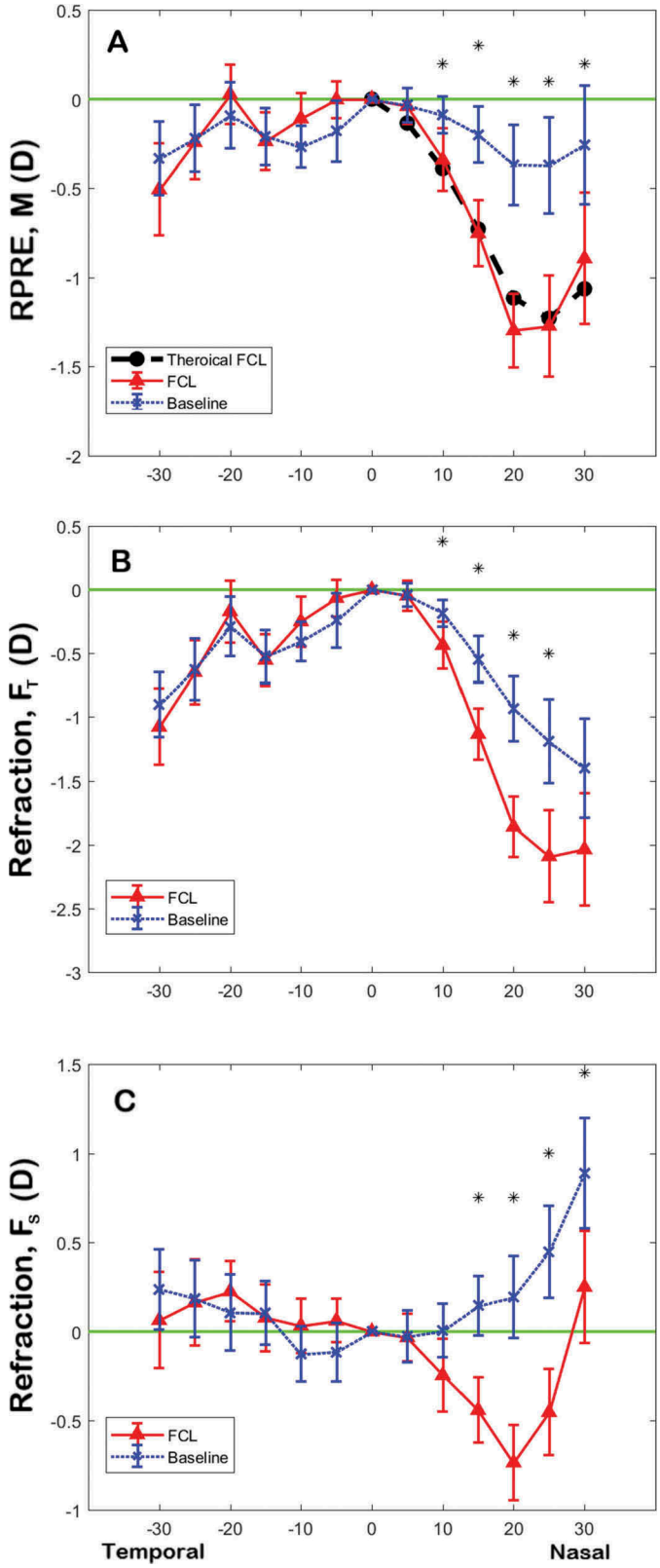

Figure 6. A, Mean values of the spherical equivalent M (RPRE) along the horizontal visual field in the naked eye (Baseline) and with Fractal Contact Lenses (FCL) The black symbols and dashed line represent the theoretical values computed by ray tracing (see the main text for details). B, Tangential, and C, Sagittal powers along the horizontal retina in the baseline state and with FCLs. Asterisks mark positions where the difference between both curves are statistically significant ($p < 0.05$).

minor changes are induced by the lens that can only be appreciated in oblique meridians.

Declaration of interests

M. Rodríguez-Vallejo, J. A. Monsoriu and W. D. Furlan are inventors: ES Patent P201330862, relating to contact lens design: assigned to Universidad Politécnica de Valencia and Universitat de Valéncia.
D. Montagud and V. Ferrando report no conflicts of interest.
The authors alone are responsible for the content and writing of the paper.

Funding

This work was founded by Ministerio de Economía y Competitividad FEDER (Grant DPI2015-71256-R), and by Generalitat Valenciana (Grant PROMETEOII-2014-072), Spain.

ORCID

Manuel Rodriguez-Vallejo http://orcid.org/0000-0001-5466-875X

References

1. Wolffsohn JS, Calossi A, Cho P, Gifford K, Jones L, Li M, Lipener C, Logan NS, Malet F, Matos S, et al. Global trends in myopia management attitudes and strategies in clinical practice. Cont Lens Anterior Eye. 2016;39:106–16.
2. Huang J, Wen D, Wang Q, McAlinden C, Flitcroft I, Chen H, Saw SM, Chen H, Bao F, Zhao Y, et al. Efficacy comparison of 16 interventions for myopia control in children. Ophthalmology. 2016;123:697–708.
3. Walline JJ. Myopia control: A review. Eye Contact Lens. 2016;42:3–8.
4. González-Méijome JM, Faria-Ribeiro MA, Lopes-Ferreira DP, Fernandes P, Carracedo G, Queiros A. Changes in peripheral refractive profile after orthokeratology for different degrees of myopia. Curr Eye Res. 2015;41:199–207.
5. Sankaridurg P. Contact lenses to slow progression of myopia. Clin Exp Optom. 2017;100:432–43.
6. Hiraoka T, Kotsuka J, Kakita T, Okamoto F, Oshika T. Relationship between higher-order wavefront aberrations and natural progression of myopia in schoolchildren. Scientific Reports. 2017;7:7876.
7. Atchison DA, Rosén R. The possible role of peripheral refraction in development of myopia. Optom Vis Sci. 2016;93:1042–44.
8. Troilo D. The case for lens treatments in the control of myopia progression. Optom Vis Sci. 2016;93:1045–48.
9. Turnbull PR, Munro OJ, Phillips JR. Contact lens methods for clinical myopia control. Optom Vis Sci. 2016;93:1–7.
10. Rodríguez-Vallejo M, Benlloch J, Pons A, Monsoriu JA, Furlan WD. The effect of Fractal Contact Lenses on peripheral refraction in myopic model eyes. Curr Eye Res. 2014;21:1151–60.
11. Charman WN. Keeping the world in focus: how might this be achieved? Optom Vis Sci. 2011;88:373–76.
12. Kee CS, Hung LF, Qiao-Grider Y, Roorda A, Smith EL. Effects of optically imposed astigmatism on emmetropization in infant monkeys. Invest Ophthalmol Vis Sci. 2004;45:1647–59.
13. Chu CH, Kee CS. Effects of optically imposed astigmatism on early eye growth in chicks. PLoS One. 2015;10:e0117729.
14. Monsoriu JA, Saavedra G, Furlan WD. Fractal zone plates with variable lacunarity. Opt Express. 2004;12:4227–34.
15. Rodríguez-Vallejo M, Montagud D, Monsoriu JA, Furlan WD. On the power profiles of contact lenses measured with NIMO TR1504. J Optom. 2017;10:265–66.

16. Plainis S, Atchison DA, Charman WN. Power profiles of multifocal contact lenses and their interpretation (Appendix A). Optom Vis Sci. 2013;90:1066–77.
17. Calossi A. Corneal asphericity and spherical aberration. J Refract Surg. 2007;23:505–14.
18. Lopes-Ferreira DP, Neves HIF, Faria-Ribeiro M, Queirós A, Fernandes PRB, González-Méijome JM. Peripheral refraction with eye and head rotation with contact lenses. Cont Lens Anterior Eye. 2014;38:104–09.
19. Thibos LN, Wheeler W, Horner D. Power vectors: an application of Fourier analysis to the description and statistical analysis of refractive error. Optom Vis Sci. 1997;74:367–75.
20. Ehsaei A, Mallen EA, Chisholm CM, Pacey IE. Cross-sectional sample of peripheral refraction in four meridians in myopes and emmetropes. Invest Ophthalmol Vis Sci. 2011;52:7574–85.
21. Osuagwu UL, Suheimat M, Atchison DA. Peripheral aberrations in adult hyperopes, emmetropes and myopes. Ophthalmic Physiol Opt. 2017;37:151–59.
22. Verkicharla PK, Suheimat M, Schmid KL, Atchison DA. Peripheral refraction, peripheral eye length, and retinal shape in myopia. Optom Vis Sci. 2016;93:1072–78.
23. Atchison DA. Optical models for human myopic eyes. Vis Res. 2006;46:2236–50.
24. He JC. Theoretical model of the contributions of corneal asphericity and anterior chamber depth to peripheral wavefront aberrations. Ophthalmic Physiol Opt. 2014;34:321–30.
25. Osuagwu UL, Suheimat M, Atchison DA. Mirror symmetry of peripheral monochromatic aberrations in fellow eyes of isomyopes and anisomyopes. Investig Opthalmology Vis Sci. 2016;57:3422–27.
26. Shen J, Clark CA, Soni PS, Thibos LN. Peripheral refraction with and without contact lens correction. Optom Vis Sci. 2016;93:642–55. 1072–1078., 2010.